2,7-Bis-(1*H*-pyrrol-2-yl)ethynyl-1,8-naphthyridine: An Ultrasensitive Fluorescent Probe for Glucopyranoside

Jen-Hai Liao,[a] Chao-Tsen Chen, [a,]* He-Chun Chou,[a] Chung-Chih Cheng,[a,+] Pi-Tai Chou, [a,]* Jim-Min Fang,[a,*,#] Zdeněk Slanina,[b] and Tashin J. Chow[b]

[a]Department of Chemistry, National Taiwan University, Taipei, 106, Taiwan. [b]Institute of Chemistry, Academia Sinica, Nankang, 115, Taiwan, Republic of China

Supporting Information:

Detailed experimental procedures, absorption, fluorescence and ^{1}H NMR spectra, molecular calculations, and X-ray diffraction data (14 pages).

[+] Chung-Chih Cheng, Department of Chemistry, Fu-Jen Catholic University, No. 510, Chung Cheng Road, Shih Chuang, Taiwan.

[#] Correspondence: Prof. Jim-Min Fang, Fax: (8862)-2363-6359. E-mail: jmfang@ccms.ntu.edu.tw

Synthetic Procedures

All reactions requiring anhydrous conditions were conducted in flame-dried apparatus under an atmosphere of argon or nitrogen. Syringes and needles for the transfer of reagents were dried at 100 ^{o}C and allowed to cool in a desiccator over P_2O_5 before use. Ethers were distilled from sodium benzophenone ketyl; (chlorinated) hydrocarbons, and amines from CaH_2. Reactions were monitored by TLC using pre-coated with a 0.25 mm layer of silica gel containing a fluorescent indicator (Merck Art. 5544). Column chromatography was carried out on Kieselgel 60 (40−63 μm). Melting points are uncorrected. Chemical shifts of ^{1}H and ^{13}C NMR spectra are reported relative to $CHCl_3$ [δ_H 7.24, δ_C (central line of t) 77.0]. Coupling constants (*J*) are given in Hz. Distortionless enhancement polarization transfer (DEPT) spectra were taken to determine the types of carbon signals.

2-(Trimethylsilylethynyl)pyrrole-1-carboxylic acid *tert*-butyl ester. To a solution of 2-bromopyrrole-1-carboxylic acid *tert*-butyl ester (1.45 g, 5.92 mmol) in 1,4-dioxane (8 mL) was added triethylamine (4 mL), trimethylsilylacetylene (1.08 mL, 7.64 mmol) followed by addition of $Pd(PPh_3)_2Cl_2$ (41.2 mg) and CuI (22.7 mg) under argon. The reaction mixture was heated at 80 ^{o}C for 20 h. The mixture was cooled, diluted with 0.1 N HCl (70 mL), and extracted with Et_2O (140 mL). The organic layer was separated, washed thoroughly with saturated $NaHCO_3$ (80 mL) and water (80 mL). The organic phase was dried (Na_2SO_4), filtered and then concentrated to dryness. The brown oil was purified by flash column chromatography with elution of 2−5% EtOAc/hexane to afford the title compound (1.23 g, 79%). Pale brown oil; TLC (EtOAc/hexane (97.5:2.5)) R_f = 0.22; IR (neat) 3157, 2967, 2155, 1750, 1320 cm^{-1}; ^{1}H NMR ($CDCl_3$, 400 MHz) δ 7.23

(1 H, dd, J = 3.4, 1.8 Hz), 6.54 (1 H, dd, J = 3.4, 1.8 Hz), 6.09 (1 H, t, J = 3.4 Hz), 1.58 (9 H, s), 0.21 (9 H, s); ^{13}C NMR ($CDCl_3$, 100 MHz) δ 148.3 (C), 122.5 (CH), 122.1 (CH), 114.9 (C), 110.8 (CH), 98.0 (C), 96.6 (C), 84.4 (C), 27.9 (3 × CH_3), –0.1 (3 × CH_3); FAB-MS *m*/*z* (rel intensity) 264 (M^+ + 1); HRMS calcd for $C_{14}H_{22}NO_2Si$ (M^+ + 1) 264.1420, found 264.1418.

2-Ethynylpyrrole-1-carboxylic acid *tert*-butyl ester. A solution of 2-(trimethylsilylethynyl)pyrrole-1-carboxylic acid *tert*-butyl ester (0.76 g, 2.88 mmol) in anhydrous MeOH (15 mL) was added KF (0.60 g), and stirred at room temperature for 6 h. After concentration to dryness the residue was purified by column chromatography with elution of 2.5–5% EtOAc/hexane to give the desired product (0.46 g, 84%). Orange oil, TLC (EtOAc/hexane (95:5)) R_f = 0.30; IR (neat) 3295, 3158, 2986, 2113, 1749 cm^{-1}; ^{1}H NMR ($CDCl_3$, 300 MHz) δ 7.22 (1 H, m), 6.56 (1 H, m), 6.09 (1 H, t), 3.32 (1 H, s), 1.57 (9 H, s); ^{13}C NMR ($CDCl_3$, 75 MHz) δ 148.1 (C), 122.5 (CH), 121.8 (CH), 114.1 (C), 110.7 (CH), 84.6 (C), 81.2 (CH), 75.7 (C), 27.8 (3 × CH_3); FAB-MS *m*/*z* (rel intensity) 192 (M^+ + 1); HRMS calcd for $C_{11}H_{14}NO_2$ (M^+ + 1) 192.1025, found 192.1026.

2,7-Bis-(1-*tert*-butoxycarbonylpyrrol-2-yl)ethynyl-1,8-naphthyridine. To a suspension of 2,7-dichloro-1,8-naphthyridine (137 mg, 0.723 mmol) in anhydrous THF (2 mL) was added triethylamine (1.38 mL), $Pd(PPh_3)_2Cl_2$ (20.1 mg) and CuI (11 mg) under argon. After stirring at room temperature for 10 min, 2-ethynylpyrrole-1-carboxylic acid *tert*-butyl ester (276 mg, 1.445 mmol) in anhydrous THF (10 mL) was added slowly. The resulting red solution was stirred at room temperature for 40 h. The reaction mixture was passed through a short plug of celite, and washed with EtOAc. The combined organic phase was evaporated to dryness under reduced pressure to give pale brown solid. After washing with hot hexane the crude

product was recrystallized from EtOAc/hexane to give the title compound (189 mg). The filtrate was concentrated to dryness, and followed the previous procedure to give the second crop (97 mg). Total yield 78%. Pale brown solid, mp 170 °C (dec.); IR (KBr) 3047, 2981, 2212, 1752 cm^{-1}; ^1H NMR ($CDCl_3$, 400 MHz) δ 8.06 (2 H, d, *J* = 8.2 Hz), 7.60 (2 H, d, *J* = 8.2 Hz), 7.36 (2 H, m), 6.81 (2 H, m), 6.22 (2 H, m), 1.64 (18 H, s); ^{13}C NMR ($CDCl_3$, 100 MHz) δ 155.9 (C), 148.1 (2 × C), 147.7 (2 × C), 136.4 (2 × CH), 125.2 (2 × CH), 123.9 (2 × CH), 123.5 (2 × CH), 120.8 (C), 114.2 (2 × C), 111.5 (2 × CH), 93.1 (2 × C), 84.9 (2 × C), 77.2 (2 × C), 28.1(6 × CH_3); FAB-MS *m*/*z* (rel intensity) 509 (M^+ + 1, 100%); HRMS calcd for $C_{30}H_{29}N_4O_4$ (M^+ + 1) 509.2189, found 509.2202.

2,7-Bis-(1*H*-pyrrol-2-yl)ethynyl-1,8-naphthyridine. To a solution of 2,7-bis-(1-*tert*-butoxycarbonylpyrrol-2-yl)ethynyl-1,8-naphthyridine (100 mg, 0.197 mmol) in anhydrous THF (5 mL) was added MeONa (63.8 mg, 6 equiv) in anhydrous MeOH (5 mL). The resulting mixture was allowed to stir at room temperature for 1 h. After evaporation to dryness the residue was treated with water (30 mL) and CH_2Cl_2 (50 mL). The mixture was neutralized with 1 N HCl aqueous solution. The lower layer was separated, and the aqueous layer was extracted with another portion of CH_2Cl_2 (30 mL). The combined organic phase was dried (Na_2SO_4), filtered, and evaporated to dryness under reduced pressure. The crude product was purified by column chromatography with elution of 2.5−10% MeOH/CH_2Cl_2 to give the title compound (45 mg, 74%). Orange crystal, mp >300 °C (darken above 160 °C); TLC (MeOH/CH_2Cl_2 (9:1)) R_f = 0.57; IR (KBr) 3215, 2196, 1593 cm^{-1}; ^1H NMR (DMSO-d_6, 400 MHz) δ 11.86 (2 H, s), 8.43 (2 H, d, *J* = 8.2 Hz), 7.66 (2 H, d, *J* = 8.2 Hz), 7.00 (2 H, m), 6.67 (2 H, m), 6.19 (2 H, m); ^{13}C NMR (CD_3OD, 100 MHz) δ 156.5 (C), 149.0 (2 × C), 138.8 (2 × CH), 125.9 (2 × CH), 123.1 (2 × CH), 122.1 (C), 118.5 (2 × CH), 112.2 (2 × C), 110.4 (2 × CH), 91.6 (2 × C), 88.5 (2 × C); FAB-MS *m*/*z* (rel intensity) 309 (M^+ + 1, 43%); HRMS calcd

for $C_{20}H_{13}N_4$ ($M^+ + 1$) 309.1140, found 309.1141. Anal. Calcd for $C_{20}H_{12}N_4$: C, 77.91; H, 3.92; N, 18.17. Found: C, 77.60; H, 4.08; N, 18.07.

UV-Vis Titration of BPN with Octyl β-D-Glucopyranoside (OGU)

Figure 3 in the text shows the absorption spectra of BPN (5.4×10^{-6} M) in CH_2Cl_2 by adding various OGU concentrations (C_g): a. 0, b. 1, c. 1.5, d. 3.1, e. 8.5, f. 14.0, g. 19.4, h. 27.6, i. 54.9 equiv (1 equiv = 1.7×10^{-5} M). On the basis of 1:1 stoichiometry of BPN/OGU, the relationship between the measured absorbance A as a function of the added OGU concentration, C_g, can be expressed by $A_0/(A - A_0) = [\varepsilon_M/(\varepsilon_C - \varepsilon_M)](K_a^{-1}C_g^{-1} + 1)$ where ε_M and ε_C are molar extinction coefficients of the BPN monomer and hydrogen-bonding complex, respectively at a selected wavelength. A_0 denotes the absorbance of the free BPN at that specific wavelength.

Fluorescent Titration of BPN with Octyl β-D-Glucopyranoside

An Edinburgh FS 920 spectrophotometer was used for the fluorescence titration study (Figure 4). The fluorescence spectra (λ_{ex} = 415 nm) of BPN (1.2×10^{-5} M) were taken as a function of OGU concentrations: a. 0, b. 1, c. 1.5, d. 2.1, e. 2.6, f. 3.1, g. 8.4, h. 14.0, i. 41.1 equiv (1 equiv = 3.84×10^{-5} M). * denotes Raleigh scattering. Insert: The plot of $F_0/(F - F_0)$ at 535 nm as a function of $1/C_g$ and a best linear least square-fitting curve. The relationship between the measured fluorescence intensity F and C_g in a selected wavelength can be expressed by $F_0/(F - F_0) = [\Phi_M\varepsilon_M/(\Phi_M\varepsilon_M - \Phi_C\varepsilon_C)](K_a^{-1}C_g^{-1} + 1)$ where F_0 denotes the fluorescence intensity of free BPN. Φ_M and Φ_C are fluorescence quantum yields of the free BPN and complex, respectively, and are assumed to be constant throughout the titration. The fluorescein solution in 0.1 M NaOH having a quantum yield Φ_R of 0.9 is taken as the reference (hereafter, subscript R denotes the

reference solution). Φ_M and Φ_C values were measured by excitations at 400 and 430 nm, respectively. The values are calculated according to the equation expressed as

$$\Phi = \Phi_R(I/I_R)(OD_R/OD)(n^2/n^2_R)$$

where I is the integrated intensity, OD is the optical density, and n denotes the index of refraction, which is reported to be 1.33 and 1.42 for n_R (0.1 M NaOH) and n (CH_2Cl_2), respectively.

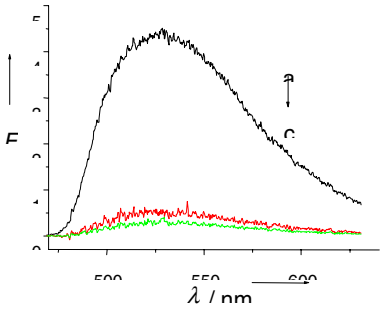

For determination of detection limit, an Ar^+ laser (465.8 nm, 30 mW, Coherent Innova 90) was used as the excitation source. The resulting luminescence was detected by an intensified charge coupled detector (ICCD, Princeton Instrument, model 576G/1) operated at a free run mode. The figure shown above is the fluorescence spectra (λ_{ex} = 465.8 nm) of BPN (1.2×10^{-5} M) as a function of OGU concentrations of **a**. 10^{-7}, **b**. 10^{-9} and **c**. 10^{-10} M. Note the emission background due to the scattering has been subtracted. Slight blue shifts of the fluorescence peak maximum (~ 530 nm) in comparison to that (535 nm) obtained by the conventional fluorescence spectrometer (Edinburgh, FS 920) are mainly due to the uncorrected spectral response in ICCD.

^{1}H NMR Titration Studies for the Binding of BPN with Monosaccharides. ^{1}H NMR spectra were measured on Brucker Avance-400 NMR spectrometer. A typical experiment was performed as follows. A solution of BPN in $CDCl_3$ was prepared (2×10^{-4} M), and a 0.4-mL portion was transferred to a 5-mm NMR tube. To the solution

was added a small aliquot of the solution containing the examined sugar in $CDCl_3$ (0.02 M). The chemical shift of N_3,N_4-H of BPN was monitored as a function of sugar concentrations. Nonlinear regression analyses were used to determine the binding constants.

Determination of the Thermodynamic Parameters for BPN/OGU Complexation.

The corresponding association constants for the BPN/OGU complex formation at variable temperatures (285, 292.5, 300 and 315 K) were deduced from the ^{1}H NMR titrations ([BPN] = 2×10^{-4} M, $CDCl_3$). A linear relationship was obtained by plotting ln$K$a as a function of 1/T according to the equation: ln$K$a = $-\Delta H/RT + \Delta S/R$. From the slope and intercept of the straight line, ΔH and ΔS were determined to be −12.3 kcal/mol and −21.8 cal/mol, respectively. ΔG was calculated to be −5.79 kcal/mol at 300 K by the equation: $\Delta G = \Delta H - T\Delta S$.

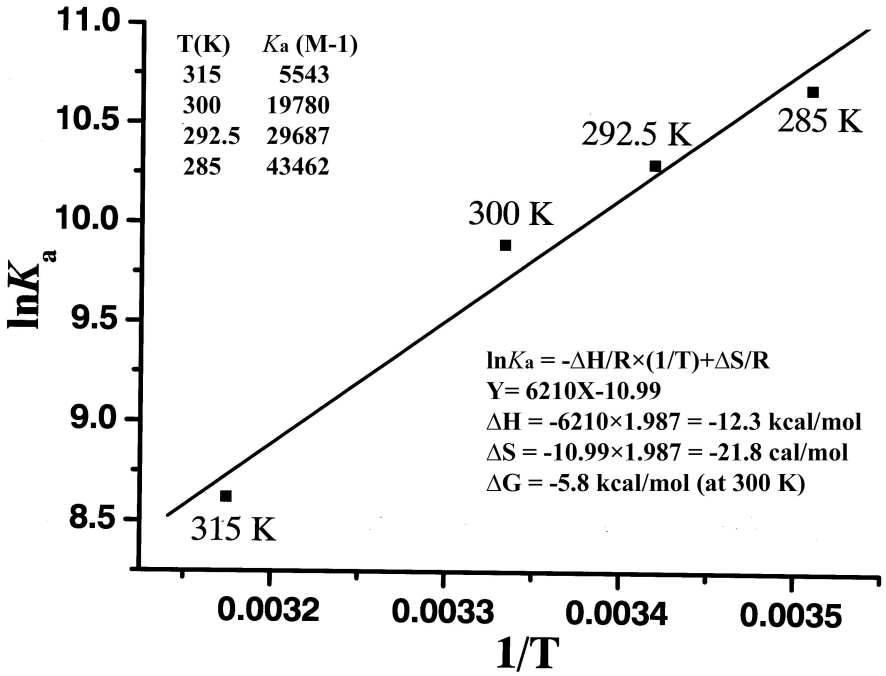

Induced ^{1}H-NMR Changes of BPN (5×10^{-4} M in $CDCl_3$, 300 K) on Addition of Monosaccharide (1 Equiv). (a): free BPN. (b): BPN with octyl β-D-glucopyranoside (OGU). (c): BPN with octyl β-D-galactopyranoside (OGA). (d): BPN with octyl

β-L-fucopyranoside (OFU).

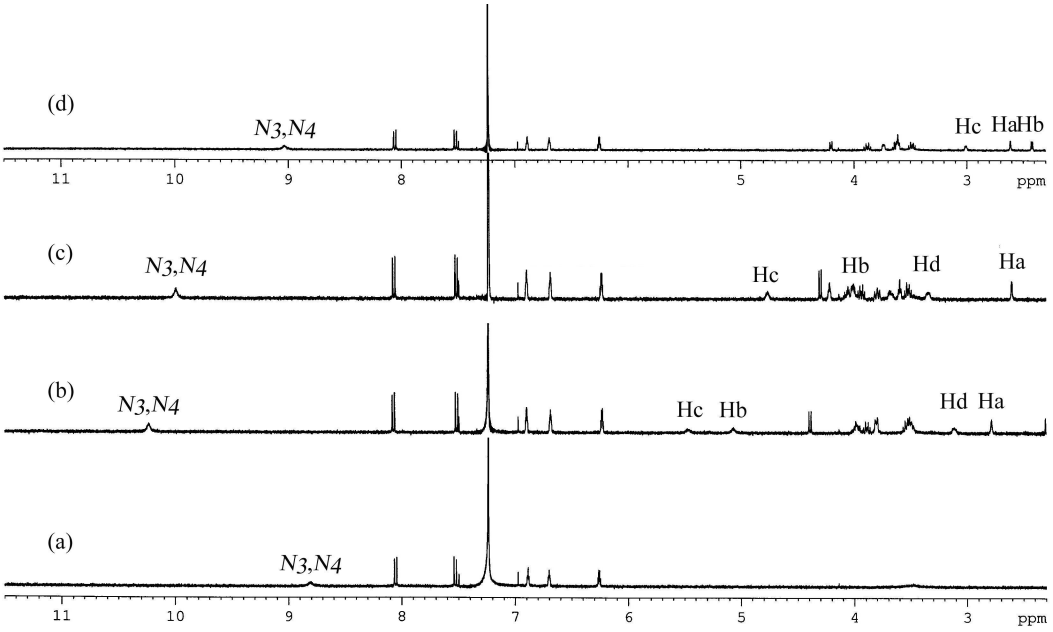

The Stoichiometry of BPN-OGU and BPN-OGA Complexes (Job Plots). Stock solutions of BPN (1×10^{-3} M) and the examined monosaccharide (1×10^{-3} M) in $CDCl_3$ were prepared in separate volumetric flasks. Nine sample solutions containing the saccharide and receptor in different molar ratios (1/1 to 9/1) were made to maintain a total volume of 0.5 mL. The chemical shift of N_3,N_4-H of BPN was monitored as a function of mole fractions of BPN. The complex concentration was calculated as follows: $[\text{complex}] = [\text{BPN}]_{tot} \times (\Delta\delta/\Delta\delta_{max})$. Both Job plots of BPN with β-D-glucopyranoside (OGU) and octyl β-D-galactopyranoside (OGA) corresponded to 1:1 stoichiometry.

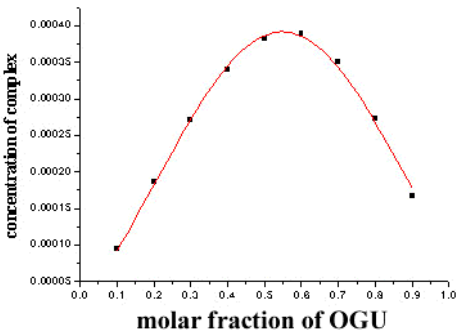
concentration of complex
0.00040
0.00035
0.00030
0.00025
0.00020
0.00015
0.00010
0.00005
0.0 0.1 0.2 0.3 0.4 0.5 0.6 0.7 0.8 0.9 1.0
molar fraction of OGU

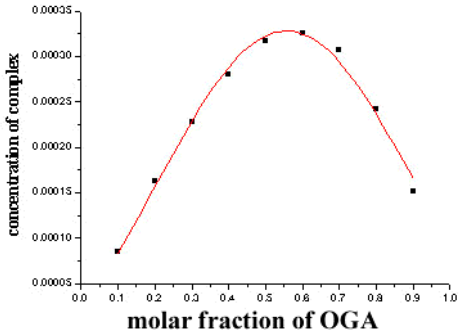
concentration of complex
0.00035
0.00030
0.00025
0.00020
0.00015
0.00010
0.00005
0.0 0.1 0.2 0.3 0.4 0.5 0.6 0.7 0.8 0.9 1.0
molar fraction of OGA

Molecular Calculations

Computations were carried out at ab initio level using selected approximations implemented in the Gaussian program package.[1] The complete geometry optimizations were performed with four increasingly more advanced methods. Three of them are ab initio Hatree-Fock (HF) methods, namely with the minimal STO-3G basis set (HF/STO-3G), with the 3-21G basis set (HF/3-21G), and with the 6-31G** basis set (HF/6-31G**). Moreover, density functional theory was also applied, namely Becke's three parameter functional with the non-local Lee-Yang-Parr correlation functional in the standard 6-31G** basis set (B3LYP/6-31G**) as the approach can, in contrast to the HF treatments, include correlation energy (with reasonable computational demands). In evaluations of the dimerization energies (E_{dim}), the basis set superposition error (BSSE) was estimated using the approximative counterpoise method.[2]

The computations indicate formation of four hydrogen bonds. The three higher-level geometry optimizations agree reasonable well, while the simple HF/STO-3G results differ significantly. At the highest level of computations, B3LYP/6-31G**, all the four computed distances are bit shorter in the glucose complex. At the same time also the computed depth of the energy minimum is slightly deeper for the glucose case in both the HF/6-31G** and B3LYP/6-31G** treatments. The relative stabilities of the two species could be still influenced by two factors not considered in our calculations - entropy and environmental effects. Moreover, the dimerization energies should be somewhat reduced by addition of the vibrational zero-point energies. In order to clarify the difference between the HF/6-31G** and B3LYP/6-31G** dimerization energies, still a higher level of theory like MP2 or even MP4 approaches would be needed, though it is too demanding on present computational resources.

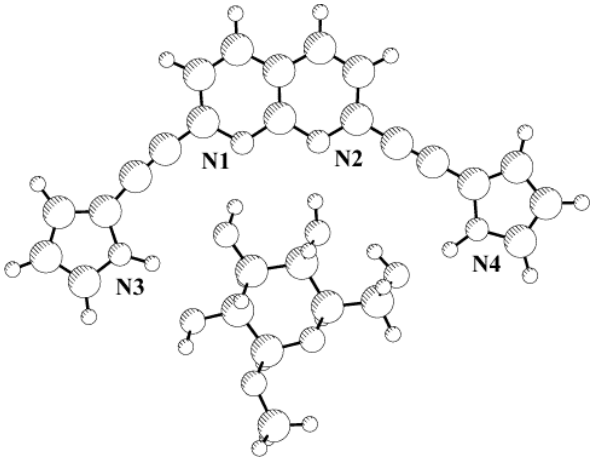

Table. Computed lengths of hydrogen bonds (in Å) and the dimerization energies ($E_{dim,}$ in kcal/mol) for the complex of BPN and methyl β-D-glucopyranoside.

method	N(1)–HO(3)	N(2)–HO(4)	N(3)H–O(2)	N(4)H–O(6)	E_{dim}
HF/STO-3G	1.810	1.773	1.674	1.467	
HF/3-21G	2.004	1.842	2.104	1.734	
HF/6-31G**	2.232	2.038	2.368	1.980	–26.19
B3LYP/6-31G**	1.970	1.827	2.140	1.813	–35.86

Table. Computed lengths of hydrogen bonds (in Å) and the dimerization energies ($E_{dim,}$ in kcal/mol) for the complex of BPN and methyl β-D-galactopyranoside.

method	N(1)–HO(3)	N(2)–HO(4)	N(3)H–O(2)	N(4)H–O(6)	E_{dim}
HF/STO-3G	1.919	1.774	1.637	1.461	
HF/3-21G	1.975	1.836	1.877	1.719	
HF/6-31G**	2.309	2.036	2.298	1.968	–25.81
B3LYP/6-31G**	2.098	1.840	2.141	1.826	–35.15

Ref. 1. Frisch, M. J.; Trucks, G. W.; Schlegel, H. B.; Scuseria, G. E.; Robb, M. A.; Cheeseman, J. R.; Zakrzewski, V. G.; Montgomery, J. A., Jr.; Stratmann, R. E.; Burant, J. C.;

Dapprich, S.; Millam, J. M.; Daniels, A. D.; Kudin, K. N.; Strain, M. C.; Farkas, O.; Tomasi, J.; Barone, V.; Cossi, M.; Cammi, R.; Mennucci, B.; Pomelli, C.; Adamo, C.; Clifford, S.; Ochterski, J.; Petersson, G. A.; Ayala, P. Y.; Cui, Q.; Morokuma, K.; Malick, D. K.; Rabuck, A. D.; Raghavachari, K.; Foresman, J. B.; Cioslowski, J.; Ortiz, J. V.; Stefanov, B. B.; Liu, G.; Liashenko, A.; Piskorz, P.; Komaromi, I.; Gomperts, R.; Martin, R. L.; Fox, D. J.; Keith, T.; Al-Laham, M. A.; Peng, C. Y.; Nanayakkara, A.; Gonzalez, C.; Challacombe, M.; Gill, P. M. W.; Johnson, B.; Chen, W.; Wong, M. W.; Andres, J. L.; Gonzalez, C.; Head-Gordon, M.; Replogle, E. S.; Pople, J. A. *GAUSSIAN 98*, Revision A.7, Gaussian, Inc., Pittsburgh, PA, 1998.

Ref. 2. Boys, S. F.; Bernardi, F. *Molec. Phys.* **1970**, *19*, 553.

X-Ray Analysis: Crystallographic data for 2,7-Bis-(l*H*-pyrrol-2-yl)ethynyl-l,8-naphthyridine (BPN) have been deposited with the Cambridge Crystallographic Data Centre as no. CCDC 176324.

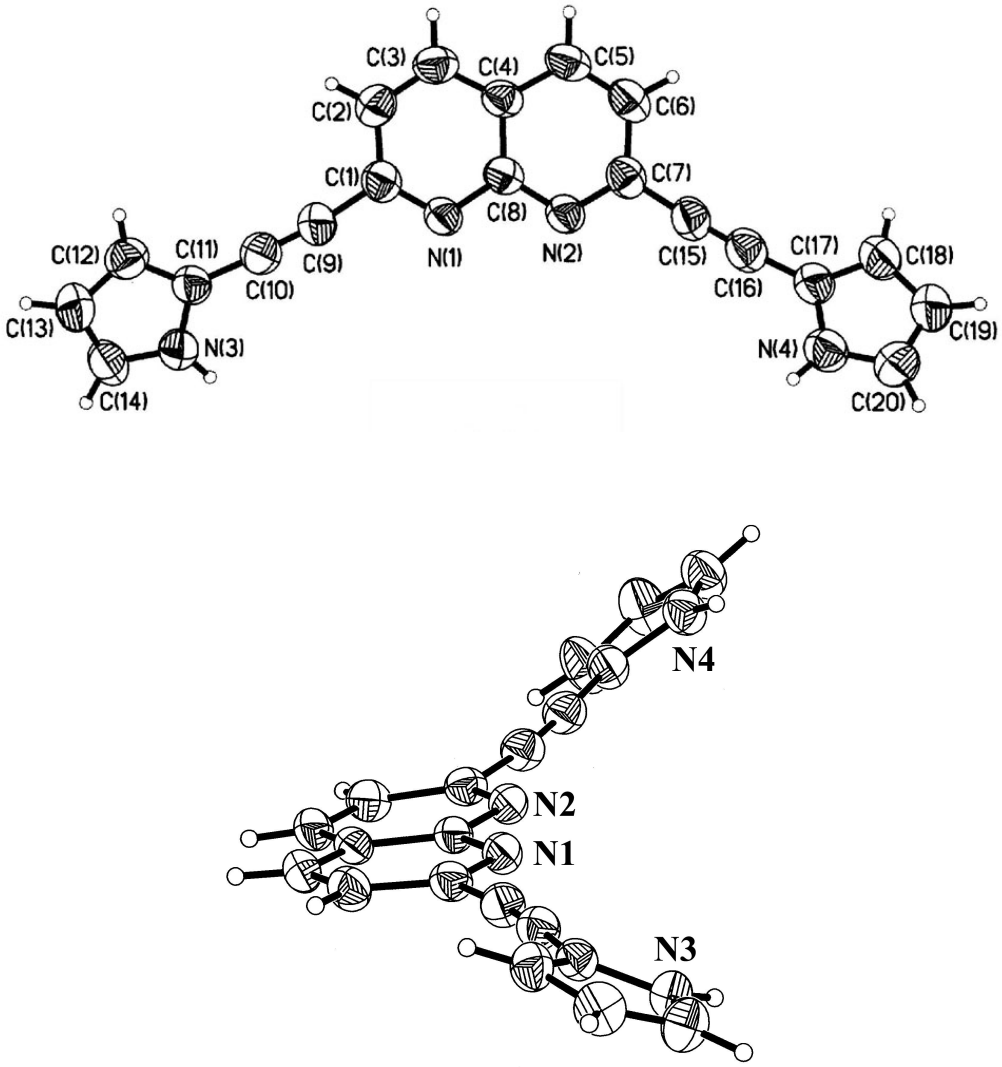

The molecular structure of BPN (IC8353) thermal ellipsoids drawn at the 50% probability level.

Table 1. Crystal data and structure refinement for ic8353. (BPN)

Identification code	ic8353
Empirical formula	$C_{20}H_{12}N_4$
Formula weight	308.34
Diffractometer used	Bruker SMART CCD
Temperature	295(2) K
Wavelength	0.71073 Å
Crystal system	Monoclinic
Space group	$P2_1/n$
Unit cell dimensions	a = 8.3452(2) Å alpha = 90° b = 12.2264(4) Å beta = 101.115(1)° c = 16.0386(5) Å gamma = 90°
Volume, Z	1605.75(8) $Å^3$, 4
Density (calculated)	1.275 Mg/m^3
Absorption coefficient	0.079 mm^{-1}
F(000)	640
Crystal size	0.50 x 0.30 x 0.20 mm
θ range for data collection	2.11 to 27.50°
Limiting indices	$-10 \le h \le 10$, $-15 \le k \le 15$, $-20 \le l \le 20$
Reflections collected	16625
Independent reflections	3681 (R_{int} = 0.0217)
Completeness to θ = 27.50°	100.0 %
Absorption correction	Semi-empirical from equivalents
Max. and min. transmission	0.9828 and 0.9050
Refinement method	Full-matrix least-squares on F^2
Data / restraints / parameters	3681 / 0 / 218
Goodness-of-fit on F^2	1.037
Final R indices [I>2σ(I)]	R1 = 0.0447, wR2 = 0.1371
R indices (all data)	R1 = 0.0759, wR2 = 0.1528
Extinction coefficient	0.003(2)
Largest diff. peak and hole	0.326 and -0.234 $eÅ^{-3}$

This structure was solved by Gene-Hsiang Lee at Instrumentation Center/NTU.

Table 2. Bond lengths [Å] and angles [°] for ic8353.

N(1)-C(1)	1.331(2)	N(1)-C(8)	1.3630(19)
N(2)-C(7)	1.332(2)	N(2)-C(8)	1.360(2)
N(3)-C(14)	1.342(2)	N(3)-C(11)	1.366(2)
N(4)-C(20)	1.344(2)	N(4)-C(17)	1.364(2)
C(1)-C(2)	1.414(3)	C(1)-C(9)	1.446(2)
C(2)-C(3)	1.352(2)	C(3)-C(4)	1.407(2)
C(4)-C(5)	1.411(2)	C(4)-C(8)	1.419(2)
C(5)-C(6)	1.354(3)	C(6)-C(7)	1.418(2)
C(7)-C(15)	1.433(3)	C(9)-C(10)	1.183(2)
C(10)-C(11)	1.421(2)	C(11)-C(12)	1.376(2)
C(12)-C(13)	1.384(3)	C(13)-C(14)	1.353(3)
C(15)-C(16)	1.195(2)	C(16)-C(17)	1.417(3)
C(17)-C(18)	1.379(3)	C(18)-C(19)	1.378(3)
C(19)-C(20)	1.353(3)		

C(1)-N(1)-C(8)	117.30(14)	C(7)-N(2)-C(8)	117.92(14)
C(14)-N(3)-C(11)	109.14(15)	C(20)-N(4)-C(17)	109.68(16)
N(1)-C(1)-C(2)	123.58(15)	N(1)-C(1)-C(9)	117.77(16)
C(2)-C(1)-C(9)	118.66(16)	C(3)-C(2)-C(1)	119.02(17)
C(2)-C(3)-C(4)	119.76(16)	C(3)-C(4)-C(5)	125.18(16)
C(3)-C(4)-C(8)	117.64(15)	C(5)-C(4)-C(8)	117.18(16)
C(6)-C(5)-C(4)	120.11(16)	C(5)-C(6)-C(7)	118.97(16)
N(2)-C(7)-C(6)	123.01(16)	N(2)-C(7)-C(15)	117.20(15)
C(6)-C(7)-C(15)	119.76(15)	N(2)-C(8)-N(1)	114.80(14)
N(2)-C(8)-C(4)	122.64(14)	N(1)-C(8)-C(4)	122.54(15)
C(10)-C(9)-C(1)	174.2(2)	C(9)-C(10)-C(11)	176.82(19)
N(3)-C(11)-C(12)	106.84(15)	N(3)-C(11)-C(10)	123.13(16)
C(12)-C(11)-C(10)	129.94(17)	C(11)-C(12)-C(13)	107.70(17)
C(14)-C(13)-C(12)	107.39(17)	N(3)-C(14)-C(13)	108.92(17)
C(16)-C(15)-C(7)	174.25(19)	C(15)-C(16)-C(17)	176.23(19)
N(4)-C(17)-C(18)	106.15(17)	N(4)-C(17)-C(16)	124.08(17)
C(18)-C(17)-C(16)	129.75(18)	C(19)-C(18)-C(17)	108.15(19)
C(20)-C(19)-C(18)	107.48(19)	N(4)-C(20)-C(19)	108.47(18)

Symmetry transformations used to generate equivalent atoms: